

# Isolation of sea urchin egg microtubules with taxol and identification of mitotic spindle microtubule-associated proteins with monoclonal antibodies

(hybridoma/immunofluorescence microscopy/immunoblot/fertilization/development)

RICHARD B. VALLEE AND GEORGE S. BLOOM

Cell Biology Group, Worcester Foundation for Experimental Biology, 222 Maple Avenue, Shrewsbury, MA 01545

Communicated by Keith R. Porter, July 11, 1983

**ABSTRACT** Microtubules were isolated from unfertilized eggs of the sea urchin with the use of the anti-tumor drug taxol. In addition to tubulin, prominent high molecular weight ( $M_r$ , 205,000–350,000) microtubule-associated proteins (MAPs) were identified as well as MAP species of  $M_r$ s 77,000, 100,000, and 120,000. The microtubules were covered with both short periodic arms and longer filamentous arms, both classes of which appeared to crosslink the microtubules into bundles. Monoclonal antibodies were prepared to an unfractionated MAPs preparation. We isolated clonal hybridoma lines producing antibodies to tubulin and to four non-tubulin proteins of  $M_r$ s 235,000, 205,000, 150,000, and 37,000. All antibodies strongly and specifically stained the mitotic spindle of dividing sea urchin eggs. All four of the immunoreactive, non-tubulin species behaved as MAPs during microtubule isolation. Thus, we have identified a variety of sea urchin MAPs by biochemical, ultrastructural, and immunochemical means. The immunochemical experiments demonstrated that four of these proteins are microtubule-associated components of the mitotic spindle. We suggest that those proteins that we observed as cross-bridges between the isolated microtubules may be either structural or functional components of the spindle.

Cytoplasmic microtubules are involved in a number of fundamental processes in eukaryotic cells. Although the question of how microtubules assemble and become organized into the variety of arrangements that have been observed in cells has been the subject of much recent work, little is known about how microtubules perform their cellular functions. The most basic role for microtubules is in cell division. Microtubules have long been known to be the predominant structural components of the mitotic spindle (1). Nevertheless, their precise role in the mechanism of mitosis is still poorly understood.

Sea urchin eggs provide an attractive experimental system for the study of mitosis. Homogeneous populations of synchronously dividing eggs can be obtained readily in large amounts sufficient for biochemical analysis. Mitosis may be monitored readily and the mitotic spindles may be manipulated experimentally *in vivo*. The primary function of microtubules in this system is in mitosis (see ref. 2); thus, the biochemical analysis of sea urchin egg microtubules should provide a relatively direct route for the molecular analysis of the mitotic spindle.

Several studies that have appeared have sought to characterize the protein components of sea urchin egg microtubules *in vitro*. Kane (3) found that microtubules would not self-assemble readily from extracts of sea urchin eggs under conditions that were used for the purification of vertebrate brain microtubules. Kuriyama (4) succeeded in assembling and purifying microtubules from sea urchin eggs after chromatographic frac-

tionation of the egg cytosolic extract. The purified microtubules contained only tubulin, the major component of microtubules. Keller and Rebhun (5) succeeded in assembling and purifying microtubules, using sea urchin mitotic spindles as starting material. In addition to tubulin, the purified microtubules contained a protein of  $M_r$  80,000. This protein potentially represented a microtubule-associated protein (MAP), though no other proteins similar to those identified in mammalian brain tissue or cultured cells (for review, see ref. 6) were observed. In addition, the microtubules were smooth-walled, lacking the fine filamentous arms characteristic of the high molecular weight mammalian brain proteins MAP 2 (7, 8) or MAP 1 (9) or the heavier arms characteristic of ciliary or flagellar dynein (10).

We sought to identify proteins associated with sea urchin microtubules with the ultimate goal of identifying microtubule-associated components of the mitotic spindle. We report here on the isolation of MAP-containing microtubules from sea urchin eggs, using a procedure (11) that takes advantage of the microtubule assembly-promoting activity of the anti-tumor drug taxol. The microtubules are covered with fine arms that resemble similar features observed in sea urchin mitotic spindles. We raised monoclonal antibodies to the MAPs and used these antibodies to demonstrate directly the presence of four distinct MAPs in the mitotic spindle.

## MATERIALS AND METHODS

**Preparation of Microtubules and MAPs.** Microtubules and MAPs were prepared by using a modification of the taxol-dependent procedure described previously (11). Unfertilized sea urchin eggs were dejellied by passage through a Nitex screen and were washed three times with  $>5$  vol of lysis buffer (0.1 M Pipes, pH 6.6/5 mM EGTA/1 mM  $MgSO_4$ /0.9 M glycerol or 0.5 M mannitol/2 mM phenylmethylsulfonyl fluoride/1 mM dithiothreitol/100  $\mu$ g of soybean trypsin inhibitor per ml). The eggs were resuspended to 3 vol in lysis buffer, homogenized in a Dounce tissue grinder, and centrifuged at  $30,000 \times g$  for 30 min at 2°C. The supernate was recovered and centrifuged at  $135,000 \times g$  for 90 min at 2°C. Taxol was added to this second supernate (cytosolic extract) to 20  $\mu$ M, and GTP was added to 1.0 mM. The cytosolic extract was warmed to 37°C for 5 min to assemble microtubules, chilled on ice for 15 min, and centrifuged at  $22,500 \times g$  for 30 min at 2°C through a cushion of 10% sucrose in lysis buffer containing 20  $\mu$ M taxol and 1.0 mM GTP. As described previously (11), the microtubule pellet was resuspended (total volume, 1/4 to 1/5 the volume of the cytosolic extract solution) and washed in 0.1 M Pipes, pH 6.6/1 mM EGTA/1 mM  $MgSO_4$  (PEM buffer) containing 1 mM GTP

Abbreviation: MAP, microtubule-associated protein.

The publication costs of this article were defrayed in part by page charge payment. This article must therefore be hereby marked "advertisement" in accordance with 18 U.S.C. §1734 solely to indicate this fact.

and 20  $\mu$ M taxol, and MAPs were dissociated from the microtubules by addition of NaCl to 0.35 M.

To obtain purified sea urchin tubulin, the following procedure was devised. We found that the MAP-free microtubules could be disassembled by resuspension in PEM buffer containing 1.0 M NaCl and lacking taxol, followed by incubation on ice for 30 min. The preparation was centrifuged at  $22,500 \times g$  for 30 min to remove a small amount of residual polymer. The tubulin was diluted 1:4 into PEM buffer and was then purified by DEAE-Sephadex chromatography (12).

**Electron Microscopy.** Microtubules were centrifuged at  $22,500 \times g$  for 20 min at  $2^\circ\text{C}$ . The pellet was fixed with 2% glutaraldehyde and 1% tannic acid and was prepared for electron microscopy as described (9).

**Preparation and Characterization of Monoclonal Antibodies.** MAPs prepared from *Lytechinus variegatus* (as in Fig. 1, lane 6) were emulsified in Freund's complete adjuvant and injected subcutaneously into a BALB/c mouse. The mouse was injected again with the MAPs antigen subcutaneously at 1 month and intraperitoneally at 6 wk. Three days after the final injection, immune splenic lymphocytes were collected and fused (13) with P3-NS1/1-Ag4-1 mouse myeloma cells in RPMI 1640 medium (GIBCO) containing 37% (wt/vol) polyethylene glycol 1000 (Koch-Lite) and 5% (vol/vol) dimethyl sulfoxide (Sigma). Cells were plated into 91 18-mm diameter culture wells and were maintained in hypoxanthine/aminopterin/thymidine selective medium from 24 hr to 2 wk after fusion. Cells were cloned in 96-well tissue culture dishes (Falcon) by limiting dilution.

Antibody production was assayed by immunofluorescence microscopy (see below). Culture fluid from 57 of the original 91 wells produced antibody that specifically stained the mitotic spindle of *L. variegatus*. Cells from eight wells were cloned, and the culture medium was assayed again by immunofluorescence microscopy for spindle staining. Culture fluid from the positive clones was used for immunoblot analysis of sea urchin egg microtubule proteins (see below) to determine the identity of the immunoreactive proteins recognized by the antibodies. Positive colonies were subcloned until all colonies produced antibody to the same antigen. One of the subclones in each case was preserved and named according to the species, molecular weight or protein name, and order of isolation. Thus, for example, L.v.37-1 was the first clone isolated that produced antibody to a  $M_r$  37,000 protein from *L. variegatus*.

Antibody isotype was determined by double immunodiffusion (14) with isotype-specific antibodies obtained from Bionetics Laboratory Products (Kensington, MD).

**Immunofluorescence Microscopy.** *L. variegatus* eggs were attached to glass coverslips coated with poly(L-lysine) (Sigma) at 5–10 mg/ml and fixed during the first or second mitotic division at  $-20^\circ\text{C}$  in methanol containing 50 mM EGTA (pH 6.0) (2). For some experiments, the coverslip-attached eggs were extracted for 2–4 min prior to fixation in PEM buffer containing 0.25% Nonidet P-40, 0.1 mg of soybean trypsin inhibitor per ml, and 2 mM phenylmethylsulfonyl fluoride. Cells were exposed to conditioned hybridoma culture medium for 1.5 hr at  $37^\circ\text{C}$ , washed in phosphate-buffered saline, and then exposed for 1.5 hr to fluorescein-conjugated sheep anti-mouse IgG prepared in this laboratory. Other steps were as described (15).

**Biochemical Analysis.** NaDodSO<sub>4</sub> gel electrophoresis was performed with 7% or 9% polyacrylamide slab gels (16). Standards for molecular weight determinations were MAP 1, MAP 2, myosin,  $\beta$ -galactosidase,  $\alpha$ -actinin, phosphorylase A, bovine serum albumin, tubulin, actin, MAP-2 assembly-promoting fragments (17), and  $\alpha$ -chymotrypsinogen. Immunoblot analysis (18) was performed as described earlier under conditions de-

signed to allow efficient transfer of high molecular weight polypeptides (15). The second antibody was peroxidase-conjugated IgG fraction of sheep antimouse IgG (Cappel Laboratories, Cochranville, PA), and the distribution of immunoreactive protein was visualized by reaction of the peroxidase with 4-chloro-1-naphthol (19).

## RESULTS

**Isolation of Sea Urchin Egg Microtubules.** The taxol-dependent procedure developed in this laboratory for isolating microtubules (11) allows for wide latitude in the choice of microtubule isolation conditions. For the present investigation, we selected conditions to minimize actin assembly (3), to promote tubulin assembly, which did not occur in the absence of taxol (cf. ref. 4), and to minimize proteolysis, which we found to be a problem with this system. The stages in the isolation of microtubules from unfertilized eggs of the sea urchin *L. variegatus* are shown in Fig. 1A. The first microtubule pellet is shown in lane 3. Tubulin was highly enriched in the pellet, while actin was greatly diminished relative to its concentration in the extract (lane 1). In addition to tubulin, a series of proteins of higher molecular weight were enriched in the first microtubule pellet. Prominent among these was a species of  $M_r$  77,000, possibly equivalent to a protein of similar molecular weight ( $M_r$  80,000) identified by Keller and Rebhun (5) in sea urchin spindle microtubule preparations. Also prominent in our preparations was a group of proteins of high molecular weight ( $M_r \approx 200,000$ – $350,000$ ). In addition to these bands, a protein of  $M_r$  100,000 and numerous minor species were noted. None of

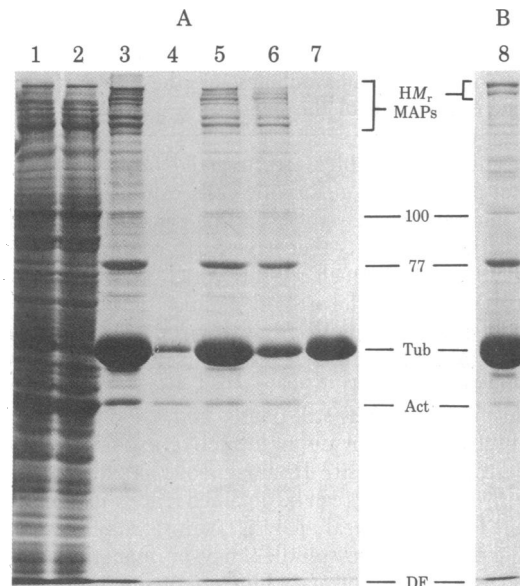


FIG. 1. Stages in sea urchin egg microtubule preparation. Microtubules were isolated by a modification of the taxol procedure (11) from cytosolic extracts of unfertilized eggs of *L. variegatus* (A) and *Strongylocentrotus purpuratus* (B): cytosolic extract (lane 1), microtubule-depleted supernatant (lane 2), and microtubule pellet (lane 3). Microtubules were resuspended in taxol-containing buffer and resedimented, giving supernatant (lane 4) and microtubule pellet (lane 5). Microtubules were resuspended in taxol-containing buffer with 0.35 M NaCl to dissociate the MAPs (11) and then were resedimented, giving MAP-containing supernatant (lane 6) and tubulin-containing microtubule pellet (lane 7). Lane 8 contains the second microtubule pellet from unfertilized eggs of *S. purpuratus*. Samples in lanes 3–8 were concentrated 25-fold relative to those in lanes 1 and 2. Molecular weights of electrophoretic bands are shown  $\times 10^{-3}$ .  $HM_r$ , high molecular weight MAPs; Tub, tubulin; Act, actin; DF, dye front.

these (except actin) appeared to represent cytosolic contaminants because they were not released when the microtubules were resuspended in taxol-containing buffer and repelleted (lanes 4 and 5). In addition, we found that in the absence of taxol, only a trace pellet was obtained in what would have been the first microtubule pellet, and none of the proteins seen in lane 3 were detectable (data not shown). These experiments suggest that the nontubulin proteins identified in lanes 3 and 5 are specifically associated with microtubules and, therefore, may be classified as MAPs.

In earlier experiments we found that all of the known MAPs of mammalian brain tissue and HeLa cells could be displaced from taxol-stabilized microtubules by exposure to elevated concentrations of NaCl (11). This was found to be the case for the entire complement of nontubulin electrophoretic bands, both major and minor (lane 6), further supporting the conclusion that these proteins were MAPs.

Fig. 1B shows the second microtubule pellet from unfertilized eggs of the sea urchin *S. purpuratus*. The electrophoretic pattern is quite similar to that for *L. variegatus*, though some differences were noted in the high molecular weight region. A band at  $M_r$  120,000 was usually also noted in *S. purpuratus*. We do not know whether the differences observed between the two species are due to proteolytic degradation or whether they reflect evolutionary divergence between the orders represented by the two sea urchin species. [The evolutionary lines that gave rise to *L. variegatus* and *S. purpuratus* are considered to have diverged more than 60 million years ago (20).]

**Morphological Examination of Microtubules.** Fig. 2 shows microtubules prepared from eggs of *L. variegatus*. Numerous small projections were seen on virtually all of the microtubules in the preparation. Many microtubules were organized into bundles, apparently held together by short periodic bridges. Longer, fine bridges were seen also (Fig. 2 Inset).

**Antibodies to Sea Urchin Microtubule Proteins.** Because the major function of microtubules in sea urchin eggs appears to be in cell division, it seemed reasonable to assume that many of the proteins isolated in association with the egg microtubules might be associated also with microtubules in the mitotic spindle. To determine whether this were the case, we began a program of antibody production with the aim of identifying spindle MAPs by immunocytochemical methods. As a first step in this process, we immunized a mouse with MAPs (as in Fig. 1, lane 6) from unfertilized eggs of *L. variegatus*. Of the original 91 hybridoma wells, 57 produced antibody that stained the mitotic spindle. From these wells we have cloned nine hybridoma lines, each of which produces a unique monoclonal antibody. The antibodies include two sea urchin-specific anti-tubulins, two broadly crossreactive anti-tubulins, and five antibodies to four distinct sea urchin MAPs. We describe below experiments performed with four anti-MAP antibodies, each of which is of the IgG1 isotype.

Fig. 3 shows dividing sea urchin eggs exposed to culture medium from the four hybridoma lines and processed for indirect immunofluorescence microscopy. All of the antibodies reacted specifically with the mitotic spindle. Staining of spindle fibers—presumably individual microtubules or bundles of microtubules—could be detected (for example, see Fig. 3A).

Fig. 4 shows immunoblot analysis performed with the monoclonal antibodies used for immunofluorescence microscopy. On the 7% polyacrylamide gels used for this analysis, the high molecular weight microtubule proteins were resolved into four major bands (Fig. 4A). The upper two bands ran approximately at the positions of bovine brain MAP 2 and MAP 1. Each antibody was found to stain a unique *L. variegatus* band distinct from tubulin (Fig. 4B-E). Weak staining of apparent MAP frag-

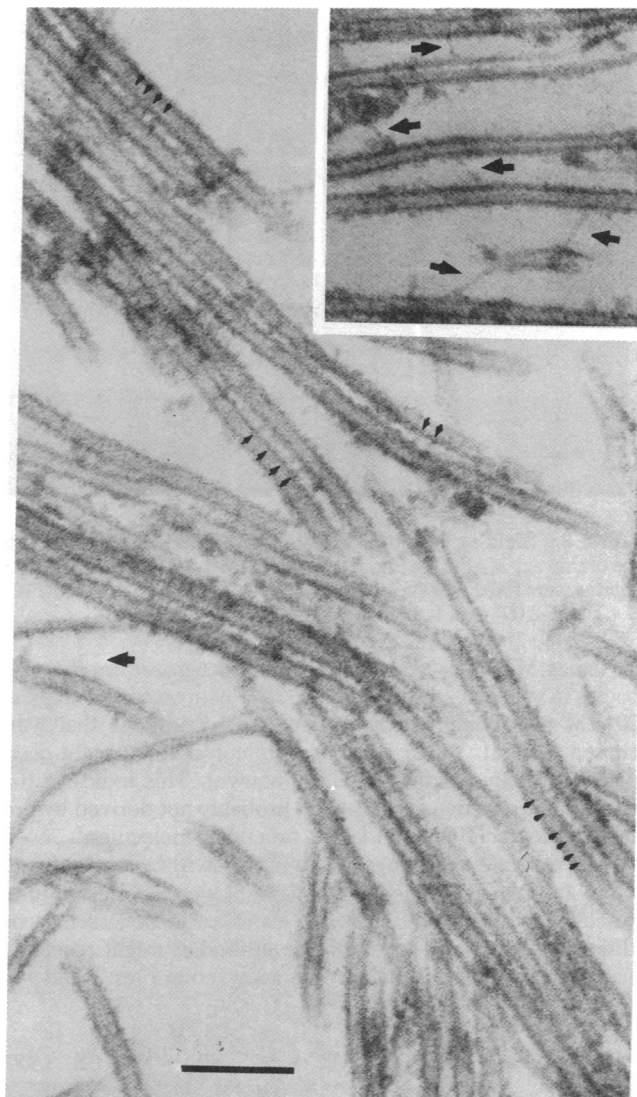


FIG. 2. Arms on sea urchin egg microtubules. Microtubules were prepared (as in Fig. 1, lane 5) from unfertilized eggs of *L. variegatus* and were examined by thin-section electron microscopy. Numerous discrete bundles of microtubules were observed. Many microtubules appeared to be connected by short, periodic crosslinking arms (small arrowheads). Fine, long, crosslinking fibers were also seen (large arrowheads). (Inset) Several of these longer fibers are shown. (Bar = 100 nm.)

ments could be detected in the microtubule pellets (lanes MT in B, C, and D). Two antibodies—termed L.v.HMW-1 and L.v.HMW-2—stained major high molecular weight MAP bands of  $M_r$  235,000 and  $M_r$  205,000, respectively, which were also identified by Coomassie blue staining. Two other antibodies—L.v.150-1 and L.v.37-1—stained less prominent bands of  $M_r$  150,000 and  $M_r$  37,000, respectively. The  $M_r$  37,000 species was barely detectable by Coomassie blue staining even on heavily loaded gels, whereas the  $M_r$  150,000 species was somewhat more prominent.

To provide further confirmation that the immunoreactive species were MAPs, immunoblot analysis was performed (Fig. 4B-E) on samples representing the initial stages in the isolation of microtubules from *L. variegatus* egg cytosol (corresponding to lanes 1-3 of Fig. 1A). All four immunoreactive species were detectable in the egg cytosolic extract (Fig. 4B-E, lanes CE). They were undetectable in the microtubule-depleted supernate (lanes S), but were highly enriched in the microtubule pel-

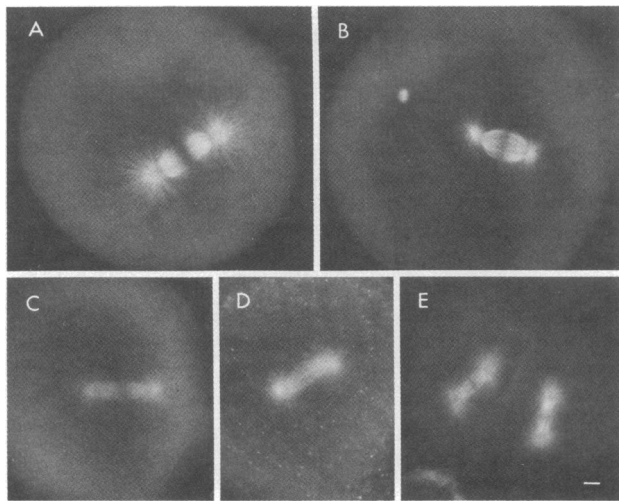


FIG. 3. Staining of mitotic spindle with monoclonal antibodies to sea urchin egg MAPs (see Fig. 4). First or second division eggs of *L. variegatus* were fixed and stained with L.v.37-1 (A and B), L.v.150-1 (C), L.v.HMW-2 (D), and L.v.HMW-1 (E). (Bar = 10  $\mu$ m.)

let (lanes MT). The same bands were recognized by the antibodies in whole eggs extracted at  $-20^{\circ}\text{C}$  with acetone containing 20  $\mu\text{M}$  phenylmethylsulfonyl fluoride, conditions that were chosen (see ref. 21) to minimize proteolysis that might occur during protein isolation (data not shown). This indicates that the immunoreactive species were probably not derived by proteolytic degradation from larger precursor molecules.

In a separate experiment (data not shown) *L. variegatus* tubulin and MAPs (as in Fig. 1A, lane 6) were spotted onto nitrocellulose paper without prior exposure to denaturing conditions to determine whether the antibodies might react with native tubulin. All four antibodies analyzed in Figs. 3 and 4 re-

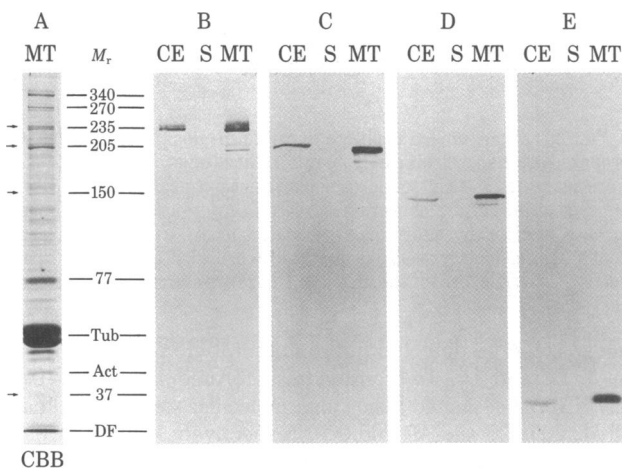


FIG. 4. Immunoblot analysis of monoclonal antibodies to sea urchin egg MAPs. (A) *L. variegatus* egg microtubules (as in Fig. 1, lane 3) were run on a 7% polyacrylamide gel and stained with Coomassie brilliant blue (CBB). (B-E) Samples from stages in microtubule isolation from unfertilized eggs of *L. variegatus* were transferred to nitrocellulose paper and stained with monoclonal antibodies: L.v.HMW-1 (B), L.v.HMW-2 (C), L.v.150-1 (D), and L.v.37-1 (E). Stages in microtubule preparation were cytosolic extract (lanes CE), microtubule-depleted supernate (lanes S), and microtubule pellet (lanes MT). Samples in lanes CE and S were prepared identically to show depletion of immunoreactive species from extract. Microtubules were concentrated 4-fold in the pellet relative to the extract or supernate. Symbols are as in Fig. 1. Arrows represent positions of immunoreactive species. Molecular weights are shown  $\times 10^{-3}$ .

acted strongly with the native MAPs fraction. None reacted with native tubulin.

Thus, by several independent criteria, the antibodies were judged to recognize multiple, distinct, nontubulin, microtubule-associated components of the sea urchin mitotic spindle.

## DISCUSSION

We succeeded in isolating microtubules from sea urchin eggs with the use of taxol. In addition to tubulin, these microtubules contained numerous other protein components (Figs. 1 and 4), most of which behaved as expected for MAPs during the taxol-dependent purification procedure (11). Four individual protein components were further judged to be MAPs with the use of monoclonal antibodies (Figs. 3 and 4). In addition, morphological evidence for the specific, periodic association of some components of our preparations with the microtubule surface was obtained (Fig. 2).

It seems reasonable to assume that some component of the high molecular weight MAPs represents the arms observed in the isolated sea urchin microtubules because, for the more extensively studied mammalian brain microtubules, the high molecular weight MAPs—MAP 2 (7, 8) and MAP 1 (9)—have been found to represent microtubule-associated arms. The fine filamentous fibers observed in our sea urchin microtubule preparations (Fig. 2 *Inset*) are in fact similar to the brain MAPs in appearance. We point out, however, that the more populous set of arms in the egg microtubule preparations appear to be shorter than the brain MAP arms and could constitute a distinct species in our preparations. This may be explained in two ways. First, it is possible that the shorter arms are composed of the  $M_r$  77,000 MAP, which appears to be the most abundant individual nontubulin polypeptide in our preparations. Therefore, this protein may represent a new category of microtubule accessory structure. Alternatively, the shorter arms could be composed of the high molecular weight MAPs but have a morphology distinct from the brain MAPs. In this context, we point out that in thin sections of axonemal preparations, dynein appears as a short, relatively indistinct protrusion (see, for example, ref. 22). Thus, it is possible that the shorter arms in our preparation represent molecules more closely related to dynein than to the major brain MAPs.

Whereas we cannot be certain yet of the molecular identity of the arms or of their role in the cell, they do seem similar in appearance to cross-bridges observed between microtubules in the mitotic spindle (23–26), in isolated kinetochore fibers (27), and in whole isolated sea urchin spindle preparations (28). Such bridges could be responsible for organizing the spindle microtubules; in addition, they may be functional elements, involved in providing the driving force for chromosome movement and for the separation of the two half spindles as proposed by McIntosh *et al.* (29).

Pratt and co-workers have recently described an enzyme present in sea urchin cytosol with enzymatic and physical characteristics similar to axonemal dynein (30, 31). Such an enzyme could be involved in the mechanochemistry of the spindle. At this time "cytoplasmic dynein" has not been proven to represent a functional component of the spindle, and it is quite possible that the enzymatic machinery of the spindle may include as yet uncharacterized molecular species. In this context, it is of interest that two of the antibodies described in this report—L.v.150-1 and L.v.37-1—recognized trace components of the sea urchin microtubule preparations (Fig. 4). The low level of the  $M_r$  37,000 and  $M_r$  150,000 components in these preparations was not due to inefficient binding to the microtubules because the proteins cosedimented quite efficiently with microtubules (Fig. 4 D and E). Thus, the concentration of available

$M_r$  37,000 and  $M_r$  150,000 proteins in egg cytosol and the content of these proteins in purified microtubules, indeed, must have been low. It is possible that these proteins will prove to be highly enriched in the spindle. We also suggest that these components may prove to be catalytic rather than structural components of the spindle. An enzymatic MAP species already has been described in brain microtubule preparations—a cAMP-dependent protein kinase associated with MAP 2 (32, 33). Enzymatic species could be present similarly in the mitotic spindle and be involved directly in mitotic movement or in the regulation of mitotic events.

It seems interesting that the MAPs that we have identified in the sea urchin mitotic spindle (Fig. 3) were originally isolated from unfertilized eggs (Figs. 1 and 4). Unfertilized eggs appear to have few, if any, assembled microtubules (2). Our results indicate that MAPs are present, therefore, prior to the onset of microtubule assembly. Why the MAPs fail to promote assembly in the unfertilized egg and whether they are involved in inducing assembly after fertilization remain topics for further investigation.

A variety of proteins have been identified in the mitotic spindle in recent years by immunocytochemical means (34–39), by selective extraction of synchronized mitotic cells (40), and by the isolation of microtubules from mitotic spindles (5, 41). Direct evidence has been presented for an involvement of only one of these proteins in mitosis (21). For many of the other proteins evaluated in these studies, the specific association with microtubules of the spindle has not been demonstrated fully yet, nor is much known about the molecular nature of these proteins. We believe that the approach we have taken in the present study offers a rapid route for conclusive identification of spindle components. Because of the large quantities of material available with the sea urchin system, we already have gained insight into the molecular properties of some of these components and, hopefully, this process will continue. The approach we have taken promises to yield a rather comprehensive sampling of the microtubule-associated components of the spindle and already suggests that the spindle is a complex organelle. This approach should be useful for the analysis of virtually any system involving microtubules and, hopefully, will yield information not only regarding mitosis but also about the variety of other cellular processes in which microtubules play a role.

We thank Drs. Kip Sluder, William Crain, and Charles Glabe of the Worcester Foundation for their interest in this work, for providing technical expertise, and for their valuable advice and suggestions. We thank Frank Luca for his excellent technical assistance. This work was supported by National Institutes of Health Grant GM 26701, March of Dimes Grant 5-388 to R.B.V., and the Mimi Aaron Greenberg Fund.

1. Porter, K. R. (1966) in *Principles of Biomolecular Organization*, CIBA Foundation Symposium, eds. Wolstenholme, F. & O'Connor, M. (Little, Brown, Boston), pp. 308–345.
2. Harris, P., Osborn, M. & Weber, K. (1980) *J. Cell Biol.* **84**, 668–679.
3. Kane, R. E. (1975) *J. Cell Biol.* **66**, 305–315.
4. Kuriyama, R. (1977) *J. Biochem. (Tokyo)* **81**, 1115–1125.
5. Keller, T. C. S. & Rebhun, L. I. (1982) *J. Cell Biol.* **93**, 788–796.
6. Vallee, R. B. (1983) in *Cell and Muscle Motility*, eds. Dowben, R. M. & Shay, J. (Plenum, New York), Vol. 5, pp. 289–311.
7. Herzog, W. & Weber, K. (1978) *Eur. J. Biochem.* **92**, 1–8.
8. Kim, H., Binder, L. & Rosenbaum, J. L. (1979) *J. Cell Biol.* **80**, 266–276.
9. Vallee, R. B. & Davis, S. E. (1983) *Proc. Natl. Acad. Sci. USA* **80**, 1342–1346.
10. Afzelius, B. (1959) *J. Biophys. Biochem. Cytol.* **5**, 269–278.
11. Vallee, R. B. (1982) *J. Cell Biol.* **92**, 435–442.
12. Vallee, R. B. & Borisy, G. G. (1978) *J. Biol. Chem.* **253**, 2834–2845.
13. Gefter, M. L., Margulies, D. H. & Scharff, M. D. (1977) *Somatic Cell Genet.* **2**, 231–236.
14. Ouchterlony, O. (1948) *Ark. Kem. Mineral. Geol.* B26:p1.
15. Bloom, G. S. & Vallee, R. B. (1983) *J. Cell Biol.* **96**, 1523–1531.
16. Laemmli, U. K. (1970) *Nature (London)* **227**, 680–685.
17. Vallee, R. B. (1980) *Proc. Natl. Acad. Sci. USA* **77**, 3206–3210.
18. Towbin, H., Staehelin, T. & Gordon, J. (1979) *Proc. Natl. Acad. Sci. USA* **76**, 4350–4354.
19. Hawkes, R., Niday, E. & Gordon, T. (1982) *Anal. Biochem.* **119**, 142–147.
20. Smith, A. B. (1981) *Palaeontology* **24**, 779–801.
21. Izant, J. G., Weatherbee, J. A. & McIntosh, J. R. (1983) *J. Cell Biol.* **96**, 424–434.
22. Witman, G. B., Plummer, J. & Sander, G. (1978) *J. Cell Biol.* **76**, 729–747.
23. Wilson, H. J. (1969) *J. Cell Biol.* **40**, 854–859.
24. Brinkley, B. R. & Cartwright, J., Jr. (1971) *J. Cell Biol.* **50**, 416–431.
25. McIntosh, J. R. (1974) *J. Cell Biol.* **61**, 166–187.
26. Inoué, S. & Ritter, H. (1975) in *Molecules and Cell Movement*, eds. Inoué, S. & Stephens, R. E. (Raven, New York), pp. 3–30.
27. Witt, P. L., Ris, H. & Borisy, G. G. (1981) *Chromosoma* **83**, 523–540.
28. Salmon, E. D. & Segall, R. R. (1980) *J. Cell Biol.* **86**, 355–365.
29. McIntosh, J. R., Hepler, P. K. & Van Wie, D. G. (1969) *Nature (London)* **224**, 659–663.
30. Pratt, M. M. (1980) *Dev. Biol.* **74**, 364–378.
31. Pratt, M. M., Otter, T. & Salmon, E. D. (1980) *J. Cell Biol.* **86**, 738–745.
32. Vallee, R. B., DiBartolomeis, M. J. & Theurkauf, W. E. (1981) *J. Cell Biol.* **90**, 568–576.
33. Theurkauf, W. E. & Vallee, R. B. (1982) *J. Biol. Chem.* **257**, 3284–3290.
34. Sherline, P. & Schiavone, K. (1978) *J. Cell Biol.* **77**, R9–R12.
35. Connolly, J. A., Kalnins, V. I., Cleveland, D. W. & Kirschner, M. W. (1977) *Proc. Natl. Acad. Sci. USA* **74**, 2437–2441.
36. Bulinski, J. C. & Borisy, G. G. (1980) *J. Cell Biol.* **87**, 792–801.
37. Browne, C. L., Lockwood, A. H., Su, J.-L., Beavo, J. A. & Steiner, A. L. (1980) *J. Cell Biol.* **87**, 336–345.
38. Welsh, M. J., Dedman, J. R., Brinkley, B. R. & Means, A. R. (1978) *Proc. Natl. Acad. Sci. USA* **75**, 1867–1871.
39. Izant, J., Weatherbee, J. A. & McIntosh, J. R. (1982) *Nature (London)* **295**, 248–250.
40. Zieve, G. & Solomon, F. (1982) *Cell* **28**, 233–242.
41. Murphy, D. B. (1980) *J. Cell Biol.* **84**, 235–245.